



# Compression behavior of ultra-high performance concrete (UHPC) confined with high-strength rectilinear ties

Wei Chang<sup>3</sup> · Wenzhong Zheng<sup>1,2,3</sup> · Meijing Hao<sup>3</sup>

Received: 23 March 2021 / Revised: 28 June 2021 / Accepted: 21 November 2021 / Published online: 13 December 2021  
© Wrocław University of Science and Technology 2021

## Abstract

To explore the compression behavior of ultra-high-performance concrete (UHPC) confined with rectilinear ties, sixty specimens were tested under axial compression. The investigated parameters included the compressive strength of UHPC in the range of 84.72–155.45 MPa, the volumetric ratio of rectilinear ties in the range of 0.9–2.0%, and the yield strength of rectilinear ties in the range of 873–1215 MPa. The failure modes of specimens were the formation of an inclined shear failure plane. The axial stress–axial strain curves and the axial stress–lateral strain curves of confined UHPC were analyzed. Besides, the effects of investigated parameters on the load-bearing capacity and ductility of confined UHPC were analyzed. Moreover, the prediction models for the lateral strain of rectilinear ties at peak stress, load-capacity and ductility of confined UHPC were developed.

**Keywords** Compression behavior · Confined UHPC · Lateral dilation · Rectilinear ties · Prediction models

## 1 Introduction

Ultra-high performance concrete (UHPC), as a new cementitious material, has been developed over two decades and has been applied to civil engineering [1]. The compressive strength of UHPC was generally over 100 MPa and even more than 150 MPa [2]. However, UHPC tended to be damaged abruptly under axial compression [3]. It was an efficient method to apply lateral confinement to UHPC to improve the ductility of UHPC [4]. The meshed rectilinear ties were the main configurations of rectilinear ties in confined concrete and the compressive behavior of UHPC confined with rectilinear ties has not been determined yet [5]. In addition, the lateral strain of rectilinear ties may not reach yield strain at

the peak stress of confined concrete [6] and the evaluation of the lateral strain of rectilinear ties has not been proposed [7]. Therefore, it was necessary to explore the compression behavior of UHPC confined with rectilinear ties.

Numerous studies have indicated that the compressive strength and ductility of concrete confined with rectilinear ties can be significantly improved. Richart studied the confinement effect of spiral stirrups on the compression behavior of concrete [8] and the prediction models for the peak stress and peak strain of confined concrete were proposed [9]. Mander explored the compression behavior of concrete confined with spiral stirrups [10] and developed the efficient confinement concept and the evaluation models of efficient confinement coefficients were proposed [11]. Saatcioglu [12], Assa [13], Li [7], and Montgomery [14] explored that the compression behavior of high-strength concrete confined with high-strength stirrups, found that high-strength concrete needed more lateral confinement than normal strength concrete and high-strength stirrups can significantly enhance the compressive strength and ductility of concrete. Baduge [15], Cusson [16], Razvi [17] indicated that high-strength lateral ties provided more lateral confinement for very-high-strength concrete (> 100 MPa) and improved ductility of confined concrete after peak stress. However, researches on the compression behavior of confined UHPC were still rare. Yang [18] explored the compression behavior of UHPC

✉ Wenzhong Zheng  
CW1558083@163.com

<sup>1</sup> Key Lab of Structures Dynamic Behavior and Control  
Ministry of Education, Harbin Institute of Technology,  
Harbin 150090, China

<sup>2</sup> Key Lab of Smart Prevention and Mitigation of Civil  
Engineering Disasters of the Ministry of Industry  
and Information Technology, Harbin Institute of Technology,  
Harbin 150090, China

<sup>3</sup> School of Civil Engineering, Harbin Institute of Technology,  
202 Haihe Road, Nangang District, Harbin, China

with 2% steel fibers in volume fraction confined with spiral stirrups with 414 MPa tensile strength and found that the peak stress and ultimate strain of UHPC were increased by 108 MPa and 1.37% in the maximum, respectively. Chen [19] found that the confinement effects on the compression behavior of UHPC confined with spiral stirrups increased obviously in the high volumetric ratio of spiral stirrups. Chang found that high-strength spiral stirrups enhanced the compressive behavior of UHPC [6].

Based on the previous studies, the existing researches mainly focused on the compression behavior of confined normal and high-strength concrete, confined UHPC with steel fibers, and UHPC confined with spiral stirrups. The lateral confinement of concrete confined with rectangular ties was lower than concrete confined with spiral stirrups at the same volumetric ratio of rectangular ties due to the decrease of the effective confinement area. Meanwhile, the lateral stress of rectangular ties at the peak stress of confined UHPC did not reach the yield strength and the lateral stress development of rectangular ties in confined UHPC has not been evaluated.

In this study, to explore the compression behavior of UHPC confined with rectangular ties, an axial compression test including 60 specimens was carried out. The failure modes, axial compression and lateral response of specimens were analyzed. Besides, the effects of the compressive strength of UHPC, the volumetric ratio and the tensile strength of rectangular ties on the compressive strength and ductility of confined UHPC were analyzed. The prediction models for the load-bearing capacity and ductility of confined UHPC and the lateral strain of rectangular ties at the peak stress of confined UHPC were developed.

## 2 Experimental program.

### 2.1 Specimens details

Sixty UHPC square columns confined with high-strength rectangular ties were designed complied with GB 50010-2010 to explore the compression behavior of confined UHPC [20]. The geometry of specimens and the design details of specimens are shown in Fig. 1a and Table 1, respectively. Grade 600 reinforcing bars with the diameter of 10 mm were applied as longitudinal reinforcement, while Grade 800, Grade 970 and Grade 1270 reinforcing bars with the diameter of 7 mm were used as rectangular ties. To prevent the damage of the end region of specimens, the spacing of rectangular ties in end region was 20 mm.

### 2.2 Materials properties

To obtain the designed UHPC, five types of compressive strength of UHPC, labeled as UHPC100, UHPC120, UHPC140, UHPC160 and UHPC180 were prepared. According to GB/T 31387-2015 [21], three  $100 \times 100 \times 100$  mm<sup>3</sup> cubes and three  $100 \times 100 \times 100$  mm<sup>3</sup> prisms of each type UHPC were tested under axial compression to obtain the mechanical properties of UHPC listed in Table 2.

Three samples for each type of reinforcing bars were tested under axial tension load according to GB/T 228-2018 [22]. The yield strength of Grade 800, Grade 970, and Grade 1270 was defined as at an offset strain of 0.2%. The mechanical properties and stress–strain curves of reinforcing bars are presented in Table 3 and Fig. 2, respectively.

**Fig. 1** Specimens geometry and test setup

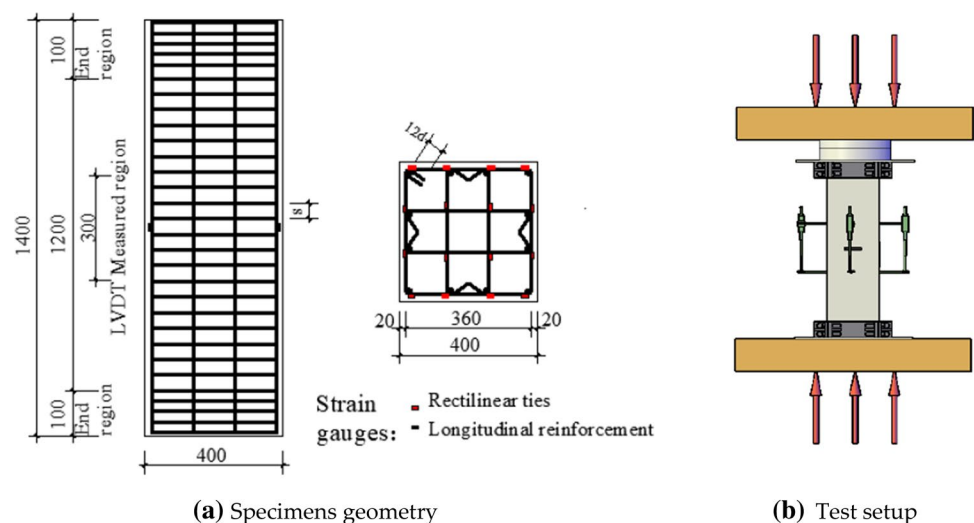


**Table 1** Specimens design details

Specimens	$f_c$ (MPa)	$f_{yv}$ (MPa)	$s$ (mm)	$d$ (mm)	$\rho_{sv}$ (%)	$\rho_{cc}$ (%)
UHPC100-800-0.9	84.72	873	95	7	0.9	0.59
UHPC100-800-1.2	84.72	873	70	7	1.2	0.59
UHPC100-800-1.4	84.72	873	60	7	1.4	0.59
UHPC100-800-2.0	84.72	873	45	7	2.0	0.59
UHPC100-970-0.9	84.72	985	95	7	0.9	0.59
UHPC100-970-1.2	84.72	985	70	7	1.2	0.59
UHPC100-970-1.4	84.72	985	60	7	1.4	0.59
UHPC100-970-2.0	84.72	985	45	7	2.0	0.59
UHPC100-1270-0.9	84.72	1215	95	7	0.9	0.59
UHPC100-1270-1.2	84.72	1215	70	7	1.2	0.59
UHPC100-1270-1.4	84.72	1215	60	7	1.4	0.59
UHPC100-1270-2.0	84.72	1215	45	7	2.0	0.59
UHPC120-800-0.9	101.66	873	95	7	0.9	0.59
UHPC120-800-1.2	101.66	873	70	7	1.2	0.59
UHPC120-800-1.4	101.66	873	60	7	1.4	0.59
UHPC120-800-2.0	101.66	873	45	7	2.0	0.59
UHPC120-970-0.9	101.66	985	95	7	0.9	0.59
UHPC120-970-1.2	101.66	985	70	7	1.2	0.59
UHPC120-970-1.4	101.66	985	60	7	1.4	0.59
UHPC120-970-2.0	101.66	985	45	7	2.0	0.59
UHPC120-1270-0.9	101.66	1215	95	7	0.9	0.59
UHPC120-1270-1.2	101.66	1215	70	7	1.2	0.59
UHPC120-1270-1.4	101.66	1215	60	7	1.4	0.59
UHPC120-1270-2.0	101.66	1215	45	7	2.0	0.59
UHPC140-800-0.9	121.81	873	95	7	0.9	0.59
UHPC140-800-1.2	121.81	873	70	7	1.2	0.59
UHPC140-800-1.4	121.81	873	60	7	1.4	0.59
UHPC140-800-2.0	121.81	873	45	7	2.0	0.59
UHPC140-970-0.9	121.81	985	95	7	0.9	0.59
UHPC140-970-1.2	121.81	985	70	7	1.2	0.59
UHPC140-970-1.4	121.81	985	60	7	1.4	0.59
UHPC140-970-2.0	121.81	985	45	7	2.0	0.59
UHPC140-1270-0.9	121.81	1215	95	7	0.9	0.59
UHPC140-1270-1.2	121.81	1215	70	7	1.2	0.59
UHPC140-1270-1.4	121.81	1215	60	7	1.4	0.59
UHPC140-1270-2.0	121.81	1215	45	7	2.0	0.59
UHPC160-800-0.9	134.47	873	95	7	0.9	0.59
UHPC160-800-1.2	134.47	873	70	7	1.2	0.59
UHPC160-800-1.4	134.47	873	60	7	1.4	0.59
UHPC160-800-2.0	134.47	873	45	7	2.0	0.59
UHPC160-970-0.9	134.47	985	95	7	0.9	0.59
UHPC160-970-1.2	134.47	985	70	7	1.2	0.59
UHPC160-970-1.4	134.47	985	60	7	1.4	0.59
UHPC160-970-2.0	134.47	985	45	7	2.0	0.59
UHPC160-1270-0.9	134.47	1215	95	7	0.9	0.59
UHPC160-1270-1.2	134.47	1215	70	7	1.2	0.59
UHPC160-1270-1.4	134.47	1215	60	7	1.4	0.59
UHPC160-1270-2.0	134.47	1215	45	7	2.0	0.59
UHPC180-800-0.9	155.45	873	95	7	0.9	0.59
UHPC180-800-1.2	155.45	873	70	7	1.2	0.59
UHPC180-800-1.4	155.45	873	60	7	1.4	0.59

**Table 1** (continued)

Specimens	$f_c$ (MPa)	$f_{yv}$ (MPa)	$s$ (mm)	$d$ (mm)	$\rho_{sv}$ (%)	$\rho_{cc}$ (%)
UHPC180-800-2.0	155.45	873	45	7	2.0	0.59
UHPC180-970-0.9	155.45	985	95	7	0.9	0.59
UHPC180-970-1.2	155.45	985	70	7	1.2	0.59
UHPC180-970-1.4	155.45	985	60	7	1.4	0.59
UHPC180-970-2.0	155.45	985	45	7	2.0	0.59
UHPC180-1270-0.9	155.45	1215	95	7	0.9	0.59
UHPC180-1270-1.2	155.45	1215	70	7	1.2	0.59
UHPC180-1270-1.4	155.45	1215	60	7	1.4	0.59
UHPC180-1270-2.0	155.45	1215	45	7	2.0	0.59

“UHPC100-800-0.9” meant that the label of UHPC-the steel type of rectilinear ties-the volumetric ratio of rectilinear ties.  $f_c$  was the compressive strength of UHPC prisms;  $s$ ,  $d$ , and  $\rho_{sv}$  were the spacing, diameter, and volumetric ratio of rectilinear ties, respectively;  $\rho_{cc}$  was longitudinal reinforcement ratio

**Table 2** Mechanical Properties of UHPC

Concrete types	$f_{cu}$ (MPa)	$f_c$ (MPa)	$\epsilon_c$ (%)	$E_c$ (MPa)	$\nu$
UHPC100	99.86	84.72	0.24	41,562	0.200
UHPC120	120.92	101.66	0.28	42,364	0.198
UHPC140	138.24	121.81	0.32	43,641	0.182
UHPC160	157.63	134.47	0.36	44,625	0.180
UHPC180	176.42	155.45	0.38	46,354	0.180

$f_{cu}$  was the compressive strength of UHPC cubes;  $f_c$  and  $\epsilon_c$  were the compressive strength and peak strain of UHPC prisms, respectively;  $E_c$  and  $\nu$  were elastic modulus and Poisson’s ratio corresponding to the average values within  $0.2f_c-0.4f_c$

**Table 3** Mechanical properties of reinforcing bars

Steel types	$f_p$ (MPa)	$f_y$ (MPa)	$f_u$ (MPa)	$E_s$ (MPa)	$\epsilon_y$ (%)
Grade 600	661	661	844	200,000	0.33
Grade 800	673	873	962	205,000	0.43
Grade 970	877	985	1089	205,000	0.48
Grade 1270	1194	1215	1400	205,000	0.59

$f_p$ ,  $f_y$ ,  $f_u$ ,  $E_s$  and  $\epsilon_y$  were the proportional limit, yield strength, ultimate strength, elastic modulus, and yield strain of steel reinforcing bars, respectively

### 2.3 Test setup

To measure the deformation of rectilinear ties, longitudinal reinforcements, concrete cover and specimens, the strain gauges and displacement meters were applied and the distributions of strain gauges and displacement meters are shown in Fig. 1. Sixteen strain gauges were placed at the corner of rectilinear ties to measure lateral strain; four strain gauges were placed on longitudinal reinforcements to measure vertical strain; two vertical and two horizontal strain gauges on the concrete cover at the middle of specimens were used to obtain vertical and horizontal strain, respectively; four

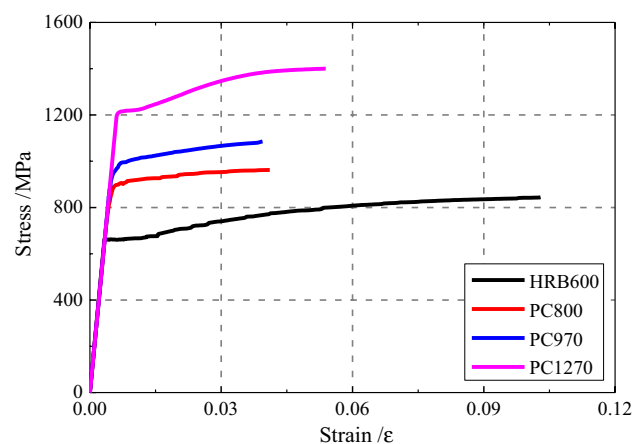


**Fig. 2** Stress–strain curves of reinforcing bars

displacement meters were placed at the middle of specimens with 300 mm regions to measure vertical deformation.

All specimens were loaded on a hydraulic testing machine with a maximum capacity of 30,000 kN at Harbin Institute of Technology. Before testing, a steel plate was installed at the two edges of specimens with 120 mm regions and high-strength cement paste was applied to the top of specimens to ensure the uniform distribution of axial load. The test setup is shown in Fig. 1b and the loading scheme of specimens with GB/T 50152-2012 [23] is listed in Table 4.

## 3 Test results and discussion

### 3.1 Observed behavior

The typical failure mode of specimens was the buckling of longitudinal reinforcement, the fracture of rectilinear ties and the formation of an inclined shear failure plane shown in Fig. 3. All specimens with the high volumetric ratio of

**Table 4** Loading scheme of specimens

Loading stages	Loading scheme
Pre-loading	Loading rate of 5 kN/s until 15% of the estimated ultimate capacity of specimens
Formal loading	First Loading rate of 5 kN/s until 70% of the estimated ultimate capacity of specimens
	Second Loading rate of 0.5 mm/min until 85% load-capacity of specimens
	Third Loading rate of 1.0 mm/min until 50% load-capacity of specimens
	Fourth Loading rate 1.5 mm/min until specimens crushed

**(a)** Buckling of longitudinal reinforcements**(b)** Fracture of rectilinear ties**(c)** Incline failure plane of specimens**Fig. 3** Failure mode of specimens

rectilinear ties and high compressive strength of UHPC damaged heavily and all specimens had high ductility [15]. The observed behavior of specimens is listed in Table 5.

### 3.2 Axial compression and lateral response

Figure 4 displayed the axial stress–axial strain curves and the axial stress–lateral strain curves of all specimens. The axial stress–axial strain curves and the axial stress–lateral strain curves of each series specimen were plotted according to the volumetric ratio of rectilinear ties. The axial strain was calculated from the average values of four vertical displacement meters divided by the gauge length (300 mm); the lateral strain was derived values from rectilinear ties; the axial stress of core concrete was obtained by subtracting the axial force of longitudinal reinforcement and concrete cover from the axial total force; the axial force of longitudinal reinforcement was calculated by the elastic modulus multiplied by the axial strain and the total cross-sectional area, when the axial stress of longitudinal reinforcement exceeded yield strength, the axial stress of longitudinal reinforcement equaled yield strength; and the axial force of concrete cover was obtained by the vertical stress multiplied by area of concrete cover; the stress–strain curves of unconfined concrete was evaluated by the models proposed by Guo [24].

The axial stress–axial strain curves of specimens had three stages: elastic stage, plastic stage and destruction stage (descending branch), corresponding to the axial stress–lateral strain curves of specimens. In the elastic stage, specimens remained the elastic behavior up to the compressive strength of unconfined UHPC, which was similar to unconfined UHPC. Meanwhile, the lateral strain of rectilinear ties was at the low level, which indicated that the lateral deformation of UHPC was due mostly to the Poisson's effect and the confinement effects of rectilinear ties were insignificant. Thus, the lateral confinements of rectilinear ties did not change the axial stress–axial strain curves of UHPC in elastic stage. The plastic stage denoted that the nonlinear behavior of confined UHPC was from the compressive strength of unconfined UHPC to the peak stress of confined UHPC. The plastic



**Table 5** Observed behavior of specimens

Loading stage	Observed behavior
Before the peak stress of unconfined UHPC	Specimens did not have obvious behavior
Around the peak stress of unconfined UHPC	Tiny hair cracks appeared on the surface at the corner of specimens; concrete cover began to spall with intermittent cracking sound
Around 80% peak stress of confined concrete	Vertical cracks were fully distributed on concrete cover; the concrete fragments on concrete cover spalling severely with continuous cracking sound; the main shear inclined cracks began to form
Around peak stress of confined concrete	Concrete cover was peeled off; the main shear inclined cracks of core concrete was formed, which divided specimens into two wedges
After peak stress of confined concrete	Two wedges were sliding over each other under monotonically increased axial load
Finally	Load-bearing capacity of specimens dropped abruptly with rectilinear ties fractures and longitudinal reinforcement buckling

behavior of specimens was induced by the lateral confinements of rectilinear ties. The lateral strain of rectilinear ties had a rapid increase due to the development of internal cracks of concrete, which demonstrated that the lateral confinements of rectilinear ties were activated. The destruction stage was marked by a gradual decrease of axial stress and the specimens with the high volumetric ratio of rectilinear ties had a stress platform. The axial stress in the stress platform increased with the increase of the volumetric ratio of rectilinear ties and decreased with the compressive strength of UHPC. Meanwhile, the lateral strain of rectilinear ties had a rapid increase until the fracture of rectilinear ties.

With the increase of the compressive strength of UHPC, the proportion of plastic behavior in the ascending branch declined and the axial stress in the descending branch declined steeply. In addition, with the increase of the volumetric ratio of rectilinear ties, the proportion of plastic behavior in the ascending branch increased and the descending branch declined gradually. Noticeably, with the increase of tensile strength of lateral ties, the ascending branch did not have obvious changes, while the stress in the descending branch declined gradually.

### 3.3 Ductility index and toughness index

The concrete confined with rectilinear ties should have enough ductility to resist the axial compression load and earthquake load. The ductility of confined concrete was related to the post-peak stress behavior which was evaluated by the ductility index  $I_{10}$  and toughness index  $T.I.$  of confined concrete.

The definitions of the ductility index [25] and toughness index [26] of confined concrete are shown in Fig. 5. The ductility index  $I_{10}$  was defined as the ratio of the area under the axial stress–axial strain curve of confined concrete up to a strain of 5.5 times yield strain to the area under the curves up to yield strain. In Fig. 5a, the yield strain of confined concrete was defined as the extrapolation of a straight line from the origin through 0.75 peak stress to a load level of

peak stress. The yield strain equaled the x-coordinate of the intersection. For perfect elastic–plastic materials,  $I_{10} = 10$ ; for perfect elastic–brittle materials,  $I_{10} = 1$ . In Fig. 5b, the toughness index was defined as the ratio of the area under axial stress–axial strain curves up to 0.02 axial strain to the area of 0.02 peak stress.

The ductility index  $I_{10}$  and toughness index  $TI$  of all specimens are listed in Table 6. Meanwhile, the peak stress, peak strain, the lateral strain of rectilinear ties at the peak stress of confined UHPC and the effective confinement ratio are also listed in Table 6.

## 3.4 Parameters analysis

### 3.4.1 Compressive strength of UHPC

The compressive strength of UHPC determined the compression behavior and lateral response of confined UHPC. The compressive strength of UHPC had two main effects: on the one hand, UHPC with high compressive strength had high cementitious materials content, which reduced the internal defects of UHPC and declined the lateral deformation ability [12]; on the other hand, with the increase of concrete strength, the effective confinement ratio ( $\rho_{sv}f_{yv}/f_c$ ) decreased with the increase of the compressive strength of UHPC [27]. Thus, the peak stress, peak strain, ductility index and toughness index of specimens, and the lateral strain of rectilinear ties decreased with the enhancement of compressive strength of UHPC. In Table 6, when the volumetric ratio and tensile strength of rectilinear ties were 1.2% and 985 MPa, respectively, the compressive strength of UHPC increased from 88.72 to 155.45 MPa, the effective confinement ratio was decreased from 0.14 to 0.06. The load-bearing capacity and ductility of confined UHPC decreased due to the decrease of effective confinement ratio. The compressive strength ratio  $f_{cc}/f_c$  and the peak strain ratio  $\epsilon_{cc}/\epsilon_c$  between confined UHPC and unconfined UHPC declined from 1.20 to 1.12 and 1.33 to 1.17, respectively. Meanwhile, the ductility

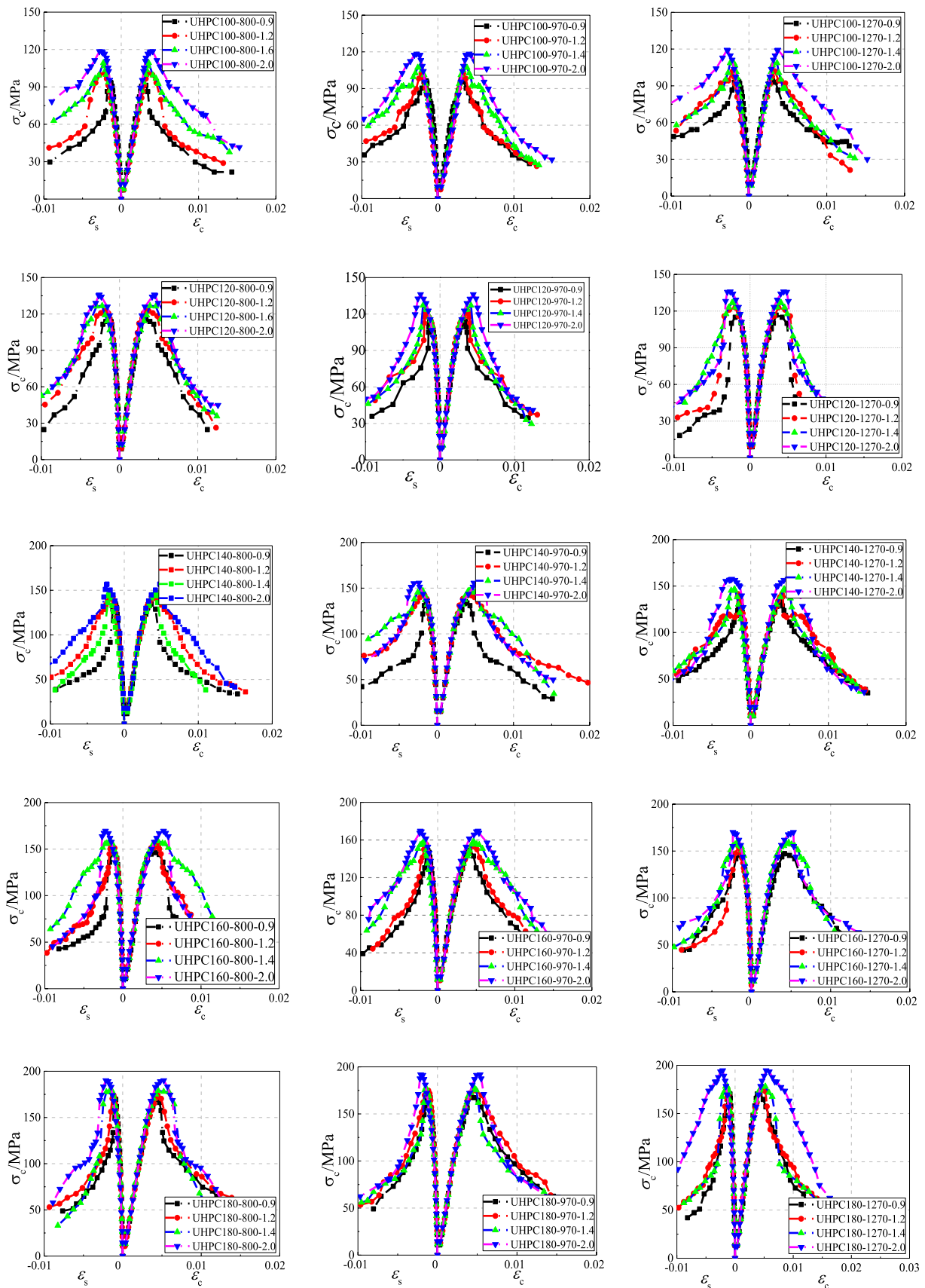
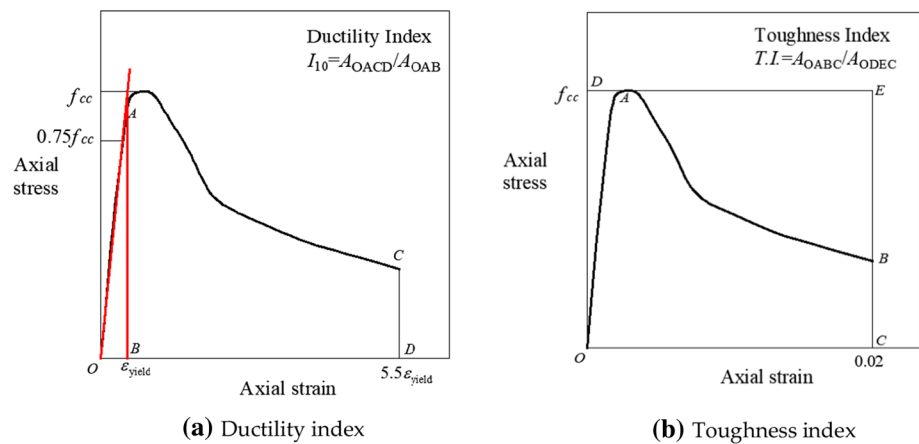


Fig. 4 Axial stress–axial strain curves and axial stress–lateral strain of confined UHPC

**Fig. 5** Definitions of ductility index and toughness index



index and toughness index were decreased from 5.24 to 5.15 and from 0.57 to 0.50, respectively. The lateral strain of rectilinear ties decreased by around  $1028 \mu\epsilon$  in the maximum.

### 3.4.2 Volumetric ratio of rectilinear ties

The volumetric ratio of rectilinear ties had two main effects on the load-bearing capacity and ductility of confined concrete: on the one hand, the effective confinement ratio increased with the increase of the volumetric ratio of rectilinear ties, which meant that more lateral confinement was provided for concrete. The lateral strain of rectilinear ties at the peak stress of confined concrete was related to the volumetric ratio of rectilinear ties [28]; on the other hand, the increase of the volumetric ratio of rectilinear ties was achieved by reducing the spacing of rectilinear ties, which restrained the buckling of longitudinal reinforcements [16]. In Table 6, when the compressive strength of UHPC was 121.81 MPa and the tensile strength of rectilinear ties was 873 MPa, the volumetric ratio of rectilinear ties increased from 0.9 to 2.0%, the effective confinement ratio was increased from 0.06 to 0.14. The compressive strength ratio  $f_{cc}/f_c$  and peak strain ratio  $\epsilon_{cc}/\epsilon_c$  between confined UHPC and unconfined UHPC increased from 1.10 to 1.29 and 1.14 to 1.50, respectively. Meanwhile, the ductility index and toughness index were increased from 4.53 to 6.15 and from 0.50 to 0.59, respectively. The high volumetric ratio of rectilinear ties enhanced the lateral expansion of concrete, which increased the lateral strain of rectilinear ties at the peak stress of confined concrete. The lateral strain of rectilinear ties increased by around  $1108 \mu\epsilon$  in the maximum.

### 3.4.3 Tensile strength of rectilinear ties

The high tensile strength of rectilinear ties enhanced the lateral confinement at a given volumetric ratio of rectilinear ties. However, high tensile strength rectilinear ties may not reach the yield strength at the peak stress of confined

concrete, which meant that tensile strength had insignificant effects on the peak stress and peak strain of confined concrete. However, high tensile strength rectilinear ties had a significant effect on the post-peak stress curves of specimens, which improved the ductility and toughness of specimens [29]. In Table 6, when the compressive strength of UHPC was 134.47 MPa and the volumetric ratio of rectilinear ties was 2.0% MPa, the tensile strength of rectilinear ties increased from 873 to 1215 MPa, the effective confinement ratio was increased from 0.11 to 0.16. The compressive strength ratio  $f_{cc}/f_c$  and peak strain ratio  $\epsilon_{cc}/\epsilon_c$  between confined UHPC and unconfined UHPC were in the range of 1.22–1.25 and 1.37–1.40, respectively, due to the insignificant lateral confinement at the peak stress of confined concrete. However, the ductility index and toughness index were increased from 5.96 to 6.65 and from 0.57 to 0.62, respectively. The high tensile strength of rectilinear ties had no obvious effects on the lateral strain of rectilinear ties at the peak stress of confined concrete. The lateral strain of rectilinear ties at the peak stress of confined UHPC was around  $2300 \mu\epsilon$ .

## 4 Load-capacity and ductility of confined UHPC

### 4.1 Effective confinement pressure of rectilinear ties

The rectilinear ties between two adjacent longitudinal reinforcements were under flexural force and tension force due to the lateral deformation of core concrete. However, the stiffness of rectilinear ties reached the maximum value at the corner of rectilinear ties or at the junction with the longitudinal reinforcements and experimental results showed that the lateral stress of rectilinear ties reached the maximum value at the maximum stiffness. Thus, the distribution of lateral



**Table 6** Experimental results of all specimens

Specimens	$f_{cc}$ (MPa)	$\epsilon_{cc}$ (%)	$\epsilon_{sv}$ (%)	$I_{10}$	T.I	$\rho_{sv}f_{sv}/f_c$
UHPC100-800-0.9	93.46	2902	1369	4.72	0.54	0.09
UHPC100-800-1.2	101.08	3465	2145	5.80	0.56	0.12
UHPC100-800-1.4	109.26	3552	2307	5.94	0.59	0.14
UHPC100-800-2.0	118.46	4080	2812	6.50	0.65	0.21
UHPC100-970-0.9	96.26	3056	1526	4.87	0.55	0.10
UHPC100-970-1.2	102.35	3356	2169	5.24	0.57	0.14
UHPC100-970-1.4	108.47	3539	2319	6.16	0.61	0.16
UHPC100-970-2.0	118.37	4102	2792	6.74	0.67	0.23
UHPC100-1270-0.9	94.35	2908	1441	4.96	0.56	0.13
UHPC100-1270-1.2	101.96	3315	2100	5.68	0.62	0.17
UHPC100-1270-1.4	108.64	3609	2416	6.38	0.65	0.20
UHPC100-1270-2.0	119.26	3724	2825	7.24	0.72	0.29
UHPC120-800-0.9	115.45	3402	1411	4.67	0.51	0.08
UHPC120-800-1.2	122.50	3738	1922	4.93	0.54	0.10
UHPC120-800-1.4	126.65	3892	2213	5.69	0.55	0.12
UHPC120-800-2.0	135.81	4468	2584	6.17	0.62	0.17
UHPC120-970-0.9	114.15	3392	1385	4.73	0.52	0.09
UHPC120-970-1.2	122.45	3739	1895	5.24	0.55	0.12
UHPC120-970-1.4	127.12	4148	2281	5.79	0.57	0.13
UHPC120-970-2.0	136.18	4463	2608	6.41	0.64	0.19
UHPC120-1270-0.9	116.72	3445	1396	4.89	0.55	0.11
UHPC120-1270-1.2	122.94	3745	1942	5.48	0.59	0.14
UHPC120-1270-1.4	126.84	3979	2255	6.13	0.62	0.17
UHPC120-1270-2.0	135.88	4426	2599	7.07	0.68	0.24
UHPC140-800-0.9	134.62	3657	1227	4.53	0.50	0.06
UHPC140-800-1.2	141.37	3946	1508	4.85	0.52	0.08
UHPC140-800-1.4	147.68	4308	2066	5.50	0.54	0.10
UHPC140-800-2.0	156.85	4793	2335	6.15	0.59	0.14
UHPC140-970-0.9	135.24	3701	1345	4.65	0.51	0.07
UHPC140-970-1.2	142.17	4012	1657	5.18	0.54	0.10
UHPC140-970-1.4	147.30	4055	2086	5.67	0.55	0.11
UHPC140-970-2.0	155.75	4796	2406	6.25	0.61	0.16
UHPC140-1270-0.9	136.07	3751	1356	4.75	0.53	0.09
UHPC140-1270-1.2	141.40	4026	1627	5.41	0.55	0.12
UHPC140-1270-1.4	146.68	4320	2112	6.04	0.58	0.14
UHPC140-1270-2.0	156.90	4971	2597	6.85	0.64	0.20
UHPC160-800-0.9	146.28	4167	1221	4.33	0.49	0.06
UHPC160-800-1.2	154.72	4466	1506	4.79	0.51	0.08
UHPC160-800-1.4	159.43	4680	1886	5.26	0.53	0.09
UHPC160-800-2.0	169.52	5203	2230	5.96	0.57	0.13
UHPC160-970-0.9	149.13	4183	1268	4.44	0.51	0.06
UHPC160-970-1.2	155.15	4503	1462	5.05	0.53	0.09
UHPC160-970-1.4	158.63	4671	1803	5.52	0.54	0.10
UHPC160-970-2.0	169.67	5236	2256	6.04	0.56	0.15
UHPC160-1270-0.9	147.25	4192	1292	4.59	0.51	0.08
UHPC160-1270-1.2	154.80	4475	1652	5.20	0.55	0.11
UHPC160-1270-1.4	159.04	4703	1850	5.44	0.57	0.13
UHPC160-1270-2.0	170.06	5304	2345	6.68	0.62	0.18
UHPC180-800-0.9	169.62	4272	940	4.24	0.47	0.05
UHPC180-800-1.2	174.05	4472	1141	4.65	0.49	0.07
UHPC180-800-1.4	178.94	4526	1364	5.04	0.50	0.08

**Table 6** (continued)

Specimens	$f_{cc}$ (MPa)	$\epsilon_{cc}$ (%)	$\epsilon_{sv}$ (%)	$I_{10}$	T.I	$\rho_{sv}f_{sv}/f_c$
UHPC180-800-2.0	190.06	5236	2143	5.73	0.54	0.11
UHPC180-970-0.9	168.89	4283	985	4.29	0.47	0.06
UHPC180-970-1.2	174.88	4461	1131	5.15	0.50	0.08
UHPC180-970-1.4	177.72	4594	1439	5.32	0.53	0.09
UHPC180-970-2.0	191.77	5368	2115	5.88	0.57	0.13
UHPC180-1270-0.9	170.92	4301	1041	4.47	0.50	0.07
UHPC180-1270-1.2	174.53	4475	1241	4.97	0.54	0.09
UHPC180-1270-1.4	178.28	4662	1360	5.10	0.55	0.11
UHPC180-1270-2.0	194.62	5326	2118	5.60	0.59	0.16

$f_{cc}$  and  $\epsilon_{cc}$  were the peak stress and peak strain of confined concrete, respectively;  $\epsilon_{sv}$  was the lateral strain of rectilinear ties at the peak stress of confined concrete;  $I_{10}$  and TI were the ductility index and toughness index of confined concrete, respectively

stress in rectilinear ties was non-uniform, and core concrete area was divided into effective confinement area and unconfined area. The effective confinement area and distribution of lateral stress for rectilinear ties are shown in Fig. 6 [30].

The maximum lateral strain of rectilinear ties was applied to calculate the lateral stress of rectilinear ties. The calculation equation of lateral stress of rectilinear ties is obtained by force balance equations shown in Eq. 1.

$$f_1 = \frac{4A_{sv}f_{sv}}{sb_{cor}} = \frac{\rho_{sv}f_{sv}}{2} \tag{1}$$

The effective confinement coefficient proposed by Mander et al. was applied to evaluate the effective confinement area by considering the effects of configurations and spacing of rectilinear ties, the distribution of longitudinal reinforcements and the dimension of the cross section of specimens. The effective confinement coefficient and the effective lateral ties are shown in Eqs. 2 and 3 [11].

$$k_e = \frac{\left(1 - \sum_{i=1}^n \frac{(b_i)^2}{6b_{cor}d_{cor}}\right) \left(1 - \frac{s'}{2b_{cor}}\right) \left(1 - \frac{s'}{2d_{cor}}\right)}{1 - \rho_{cc}} \tag{2}$$

$$f_{1e} = k_e f_1 = \frac{k_e \rho_{sv} f_{sv}}{2} \tag{3}$$

where  $s'$  is the clear space of rectilinear ties, mm;  $b_{cor}$  and  $d_{cor}$  are the width and height of core concrete, respectively, mm;  $\rho_{cc}$  is longitudinal reinforcement ratio;  $b_i$  is the distance of neighboring longitudinal reinforcement, mm;  $f_1$  is the lateral stress of rectilinear ties, MPa;  $f_{1e}$  is the effective lateral confinement of rectilinear ties, MPa.

### 4.2 Lateral strain of rectilinear ties at peak stress of confined concrete

Experimental results indicated that the lateral strain of outer rectilinear ties was larger than inner rectilinear ties. The maximum lateral strain of rectilinear ties determined effective lateral confinement, because the maximum lateral strain exceeded the rupture strain of rectilinear ties, the lateral confinement of rectilinear ties did not exist. In Table 6, the maximum lateral strain of rectilinear ties at the peak stress of confined concrete did not reach yield strain. Thus,

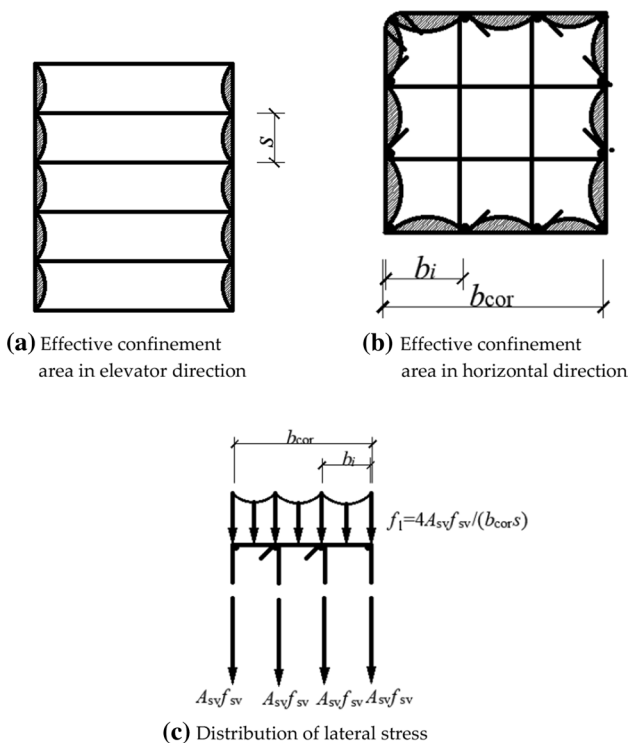


**Fig. 6** Effective confinement area and lateral stress distribution of rectilinear ties. The shadow part was the unconfined concrete area and the blank part was the effective confinement area

the actual lateral stress of rectilinear ties was applied to calculate lateral confinement.

The lateral strain of rectilinear ties at peak stress was related to the compressive strength of concrete, the elastic modulus of confining materials and the volumetric ratio of rectilinear ties [31]. The calculation model for the lateral strain of rectilinear ties was obtained by regression analysis based on the experimental results listed in Eq. 4.

$$\epsilon_{sv} = 6.64 \times 10^{-4} + 6.47 \times 10^{-5} \left( \frac{k_e E_{sv} \rho_{sv}}{f_c} \right), \quad (4)$$

where  $\epsilon_{sv}$  is the lateral strain of rectilinear ties at peak stress;  $E_{sv}$  and  $\rho_{sv}$  are the elastic modulus and volumetric ratio of rectilinear ties, respectively.

The performance of proposed models was evaluated by comparing with other prediction models. Four typical models were selected to predict the lateral strain of rectilinear ties at the peak stress of confined concrete. In Wang et al. prediction models, the lateral strain of unconfined concrete at the peak stress was taken as the minimum value equaling  $0.45E_{sv}\epsilon_c$  [28]. In Shi et al. prediction model, the effects of the volumetric ratio and configurations of rectilinear ties, the compressive strength of concrete, and the dimension of specimens were considered [31]. In Saatcioglu and Razvi prediction models, the lateral stress of rectilinear ties at the peak stress was evaluated based on experimental results by considering the effects of configurations of rectilinear ties [32]. The typical models are shown in Table 7.

Figure 7 showed that the comparison between experimental results and the prediction results from the prediction models. To enhance the prediction performance of proposed models, 17-group experimental results were collected from previous studies listed in Table 11. The Saatcioglu and Razvi model overestimated the experimental results, while Shi model underestimated the experimental

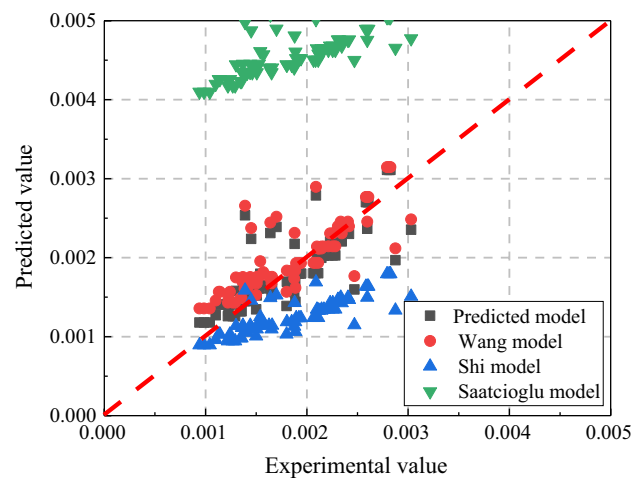


Fig. 7 Compression between experimental results and prediction results

results. Wang model and proposed model were suitable for evaluating the lateral strain of rectilinear ties at the peak stress of confined UHPC.

The prediction models for the lateral strain of rectilinear ties can be used to determine the volumetric ratio of rectilinear ties, which ensured that rectilinear ties can reach yield strength at the peak stress of confined UHPC. Let  $\epsilon_{sv} = \epsilon_{yv}$  in Eq. 4, and the volumetric ratio of rectilinear to ensure rectilinear ties reached the yield strength at the peak strength of confined UHPC was calculated by Eq. 5. The volumetric ratio of rectilinear ties for different compressive strength of UHPC was listed in Table 8.

$$[\rho_{sv}] = \frac{(\epsilon_{yv} - 6.64 \times 10^{-4})f_c}{6.47 \times 10^{-5}k_e E_{sv}} \quad (5)$$

### 4.3 Load-bearing capacity estimation

The load-bearing capacity of confined UHPC was applied to evaluate the compression behavior of confined UHPC, which was related to the peak stress of confined UHPC. According to the Mohr–Coulomb strength criterion [33], the prediction model for the peak stress of confined UHPC was proposed and is shown in Eq. 6.

Table 7 Typical prediction models for evaluating the strain of rectilinear ties at peak stress

Prediction models	Models
Wang	$\epsilon_{sv} = 12.29k\rho_v/f_c + 0.00088$
Shi	$\epsilon_{sv} = 0.378(k\rho_v/f_c)^{0.65} + 0.00038$
Saatcioglu and Razvi	$\epsilon_{sv} = 0.04(\rho_v/f_c)^{0.33} + 0.0025$

**Table 8** Volumetric ratio of rectilinear ties for different compressive strength of UHPC

Rectilinear ties	[ $\rho_{sv}$ ] (%)				
	UHPC100	UHPC120	UHPC140	UHPC160	UHPC180
Grade 800	3.32	3.98	4.77	5.27	6.09
Grade 970	3.77	4.53	5.43	5.99	6.92
Grade 1270	4.78	5.73	6.87	7.58	8.77

$k_c$  was an average value derives from the experimental results, equaled 0.7

**Table 9** Typical peak stress models

Models	Peak stress
Mander	$f_{cc} = f_c(-1.254 + 2.254\sqrt{1 + 7})$
Légeron	$f_{cc} = f_c(1 + 2.4(f_{le}/f_c)^{0.7})$
Baduge	$f_{cc} = f_c(1 + 2.7(f_{le}/f_c))$
Wei and Wu	$f_{cc} = f_c(1 + 5.35(f_{le}^{0.86}/f_c))$

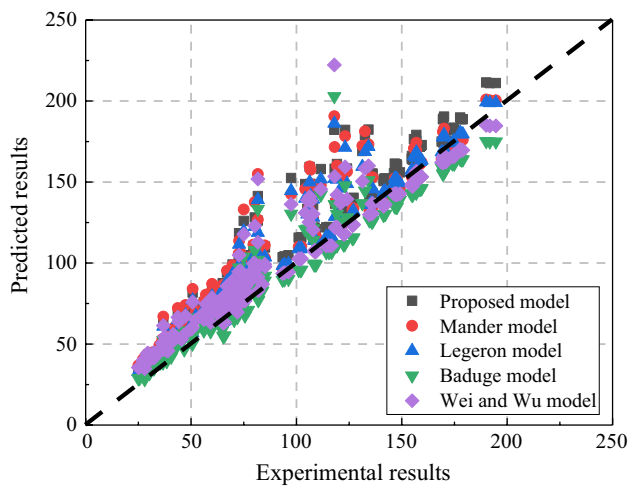


**Fig. 8** Comparison peak stress results between experiment and prediction models

$$f_{cc} = f_c \left( 1 + 2.33 (f_{le}/f_c)^{0.61} \right) \tag{6}$$

The typical prediction models for evaluating the peak stress of confined concrete were selected listed in Table 9. The model developed by Mander [11] was based on the octahedral coordinate system. The models developed by Légeron [27] were based on the strain compatibility equations and introduced the effective confinement index at peak stress. The peak stress prediction model of confined concrete was expressed as the function of the peak stress of unconfined concrete and the non-dimensional effective confinements index by regression analysis, which were suitable for the compressive strength of concrete in the range of 30–120 MPa. The peak stress prediction

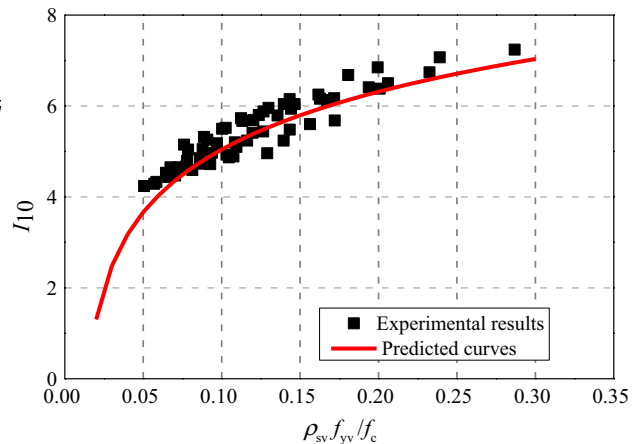


**Fig. 9** Predicted curves of prediction models for ductility index

model developed by Baduge [15] was derived from the stress–strain behavior prediction models of confined very-high-strength concrete by modifying the  $K$  value obtained by Li [7]. Wei and Wu [29] developed the prediction models for evaluating the peak stress of concrete confined with high-strength stirrups based on the Richart model [8]. Besides, 53-group experimental results were collected from the previous studies to enhance the prediction performance of proposed model, which are listed in Table 11.

Figure 8 showed that the comparison the results between experiment and prediction models. The peak stress from the proposed model was closely approximated to the experimental results, while other models underestimated the experimental results. Thus, the proposed model was a good choice to predict the peak stress of confined UHPC.

Thus, the load-bearing capacity calculation equation of confined UHPC columns by considering the lateral confinement of rectilinear ties is listed in Eq. 7.

$$N_u = f_{cc}A_{cc} + f_yA_s, \tag{7}$$

where  $A_{cc}$  and  $A_s$  were the area of core concrete and longitudinal reinforcement, respectively,  $\text{mm}^2$ ;  $f_y$  was the yield strength of longitudinal reinforcement, MPa.

**Table 10** Appropriate volumetric ratio of rectilinear ties for confined UHPC

$\rho_{sv}/\%$	UHPC100	UHPC120	UHPC140	UHPC160	UHPC180
Grade 800	1.25–13.67	1.50–16.38	1.50–19.62	1.98–21.66	2.29–25.04
Grade 970	1.11–12.10	1.33–14.51	1.59–17.39	1.75–19.20	2.03–22.19
Grade1270	0.90–9.81	1.08–11.77	1.29–14.10	1.42–15.56	1.64–17.99

#### 4.4 Ductility evaluation

The ductility of high compressive strength concrete determined the application in civil engineering. The ductility index was applied to evaluate the ductility of confined concrete. The ductility index was related to effective confinement ratio [26]. Based on the experimental results, the relationships between effective confinement ratio and ductility index are established in Eq. 8 and the curves of prediction models are shown in Fig. 9.

$$I_{10} = 1.9 \ln (142.5\rho_{sv}f_{yv}/f_c + 1.2) \quad (8)$$

The Eq. 8 can be transformed as Eq. (9).

$$1.7e^{I_{10}} = 142.5\rho_{sv}f_{yv}/f_c + 1.2 \quad (9)$$

The ductility index  $I_{10}$  of confined concrete was applied to determine the requirements of the volumetric ratio of rectilinear ties to ensure that concrete had enough ductility to resist the seismic load. Foster indicated that the  $I_{10}$  of confined concrete should be more than 8 to satisfy the requirements of low to moderate seismicity [34]. Zaina and Foster [35] revised the requirement ductility level and adjusted the requirement to  $I_{10} \geq 5.6$ . Shin [36] found that the effective confinement ratio  $\rho_{sv}f_{yv}/f_c$  should be more than  $0.109f_c$  to ensure the required ductility of confined concrete. The requirements of the volumetric ratio of rectilinear ties for confined UHPC should satisfy the requirements of both effective confinement ratio and ductility, the calculation models were expressed in Eq. 10. The appropriate volumetric ratio of rectilinear ties for confined UHPC is shown in Table 10.

$$\begin{cases} \rho_{sv}f_{yv}/f_c \geq 0.109 \\ 1.7^{5.6} \leq 142.5\rho_{sv}f_{yv}/f_c + 1.2 \leq 1.7^{10} \end{cases} \quad (10)$$

## 5 Conclusion

In this study, 60 square UHPC columns confined with rectilinear ties were tested under axial compression to evaluate the compression behavior of confined UHPC. Based on the

analysis of experimental results, the following conclusions were drawn:

1. The typical failure mode of specimens was the buckling of longitudinal reinforcement, the fracture of rectilinear ties and the formation of an inclined shear failure plane.
2. The axial stress–axial strain curves and the axial stress–lateral strain curves of specimens were divided into the elastic ascending branch, nonlinear ascending branch, and destruction stage. The nonlinear ascending branch became obvious with the increase of the volumetric ratio of rectilinear ties.
3. Concrete strength and rectilinear ties volumetric ratios enhanced the peak stress and peak strain of confined concrete, while rectilinear ties tensile strength had no obvious effects on the peak stress and peak strain. Concrete strength decreased the lateral stress of rectilinear ties at the peak stress, while the volumetric ratio of rectilinear ties enhanced lateral stress. The tensile strength of rectilinear ties had no obvious effects on the lateral stress of specimens.
4. Both the volumetric ratio and tensile strength of rectilinear ties improved the ductility of confined UHPC, while the compressive strength of UHPC had negative effects on the ductility of UHPC.
5. The prediction model for the evaluating the lateral strain of rectilinear ties at the peak stress of confined concrete was developed and the volumetric ratio of rectilinear ties to ensure that rectilinear ties reached the yield strength at the peak stress of confined concrete was given.
6. The prediction models for the load-bearing capacity and ductility of confined UHPC were established to evaluate the compression behavior of confined UHPC.

## Appendix

The experimental results were collected from previous studies to enhance the prediction performance of proposed models for the lateral strain of rectilinear ties at the peak stress and the peak stress of confined concrete, which are listed in Table 11.



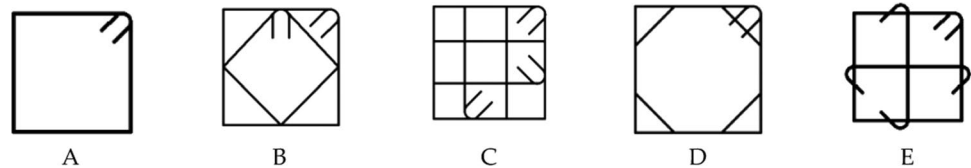
**Table 11** Collected experimental data for concrete columns confined with rectilinear ties

References	Specimens	Configurations	$f_c$ (MPa)	$f_{yv}$ (MPa)	$s$ (mm)	$d$ (mm)	$\rho_{sv}$ (%)	$\epsilon_{yv}$ (%)	$f_{cc}$ (MPa)	$\epsilon_{sv}$ (%)
[7]	1	B	60	445	20	6	4.48	0.26	80.24	Yield
	2	A	60	445	35	6	1.50	0.26	68.58	Yield
	3	A	60	445	50	6	1.05	0.26	72.17	Yield
	4	A	60	445	65	6	0.80	0.26	72.01	0.16
	5	B	60	445	65	6	1.38	0.26	72.12	0.14
	6	B	72.3	445	20	6	4.48	0.26	106.71	Yield
	7	A	72.3	445	35	6	1.50	0.26	82.45	Yield
	8	B	72.3	445	35	6	2.56	0.26	81.73	Yield
	9	A	72.3	445	50	6	1.05	0.26	83.92	0.15
	10	B	72.3	445	50	6	1.79	0.26	80.56	0.21
	11	B	72.3	445	65	6	1.38	0.26	81.76	0.19
	12	B	52	1318	20	6.4	5.00	0.85	117.99	Yield
	13	B	52	1318	35	6.4	2.86	0.85	81.71	Yield
[37]	1	A	46.3	1288	50	6.4	0.96	0.86	50.14	0.17
	2	A	46.3	1028	100	6.0	0.51	0.73	42.99	0.18
	3	A	46.3	1288	100	6.4	0.48	0.86	45.46	0.15
	4	A	84.8	1288	50	6.4	0.96	0.86	80.03	0.13
	5	A	128	1288	50	6.4	0.96	0.86	111.59	0.11
[38]	1	E	39.2	1420	150	6.4	0.55	0.71	39.1	0.19
	2	E	80.0	1420	85	6.4	0.96	0.71	85.1	0.25
	3	A	80.0	1420	40	6.4	1.20	0.71	72.8	0.29
	4	E	116.0	1420	40	6.4	2.05	0.71	123.1	0.30
	5	A	116.0	1420	40	6.4	1.20	0.71	97.5	0.19
	6	E	39.2	379	40	6	2.16	0.19	47.4	Yield
[39]	1	A	96.4	392	50	7.9	2.0	0.20	107.97	0.15
	2	D	98.1	410	100	9.5	2.6	0.20	105.95	0.16
	3	B	95.4	392	50	7.9	3.4	0.20	124.02	Yield
	4	D	95.4	392	50	7.9	3.6	0.20	119.25	Yield
	5	C	100.4	392	50	7.9	4.8	0.20	132.53	Yield
	6	B	96.4	414	50	6.4	2.2	0.20	107.97	Yield
	7	B	93.1	392	50	7.9	3.4	0.20	121.03	Yield
	8	C	93.1	392	50	7.9	4.8	0.20	131.27	Yield
	9	C	67.9	680	50	7.9	4.8	0.54	118.15	Yield
	10	B	52.6	715	50	9.5	4.9	0.55	105.20	Yield
	11	C	55.6	680	50	7.9	4.8	0.54	106.75	Yield
[40]	1	B	20.0	550	50	6	2.33	0.27	37.57	Yield
	2	C	20.0	550	70	8	3.46	0.27	44.20	Yield
	3	E	34.8	550	30	5	2.64	0.27	57.09	Yield
[41]	1	C	38.3	476	70	8	1.91	0.24	64.81	Yield
	2	C	38.3	642	70	8	1.91	0.31	66.48	Yield
	3	B	38.3	642	90	8	1.28	0.31	65.40	Yield
	4	C	38.3	642	105	8	1.28	0.31	65.38	Yield
	5	C	38.3	642	105	8	1.28	0.31	65.91	Yield
	6	C	38.3	642	70	8	1.91	0.31	70.47	Yield
[42]	1	B	45	398	120	11.3	3.43	0.20	50.77	Yield
	2	E	34	398	85	11.3	3.02	0.20	36.87	Yield
	3	D	34	398	85	11.3	3.63	0.20	43.77	Yield

**Table 11** (continued)

References	Specimens	Configurations	$f_c$ (MPa)	$f_{yv}$ (MPa)	$s$ (mm)	$d$ (mm)	$\rho_{sv}$ (%)	$\epsilon_{yv}$ (%)	$f_{cc}$ (MPa)	$\epsilon_{sv}$ (%)
[43]	1	C	124	400	120	11.3	3.06	0.2	134.2	Yield
	2	E	92	400	85	11.3	3.24	0.2	104.2	Yield
	3	C	92	400	85	11.3	4.32	0.2	106.3	Yield
	4	E	60	400	85	11.3	3.24	0.2	72.6	Yield
	5	C	60	400	120	11.3	3.06	0.2	69.7	Yield

The configuration of rectilinear ties is denoted as A, B, C, D and E, which is shown in Fig. 10

**Fig. 10** Configurations of rectangular ties

**Acknowledgements** This research was funded by the National Science Foundation of China (Grant number 51678190).

## Declarations

**Conflicts of interest** The authors declare no conflict of interest.

## References

- Azmeem NM, Shafiq N. Ultra-high performance concrete: from fundamental to applications. *Case Study Constr Mater*. 2018;9:1–12.
- Shi CJ, Wu ZM, Xiao JF, Wang DH, Huang ZY, Fang ZF. A review on ultra-high performance concrete: part I. Raw materials and mixture design. *Constr Build Mater*. 2015;101(1):741–51.
- Nematollahi B, Saifulnaz MRR, Jaafar MS, Voo YL. A review on ultra high performance ‘ductile’ concrete (UHPdC) technology. *Int J Comput Civ Struct Eng*. 2012;2(3):1003–18.
- Hoang AL, Fehling E, Lai B. Experimental study on structural performance of UHPC and UHPFRC columns confined with steel tube. *Eng Struct*. 2019;187(5):457–77.
- Deng ZC, Yao JS. Axial compression behavior of ultra-high performance concrete columns confined by high-strength stirrups. *Acta Mater Compos Sin*. 2020;37(10):2590–601.
- Chang W, Zheng WZ, Chen P. Compressive behavior of high performance concrete (HPC) and high performance fiber-reinforced concrete (HPFRC) confined with spiral stirrups. *J Mater Civ Eng*. 2021;33(4):04021034.
- Li B. Strength and ductility of reinforced concrete members and frames constructed using high strength concrete. Christchurch: Civil Engineering at the University of Canterbury; 1993.
- Richart FE, Brandtzaeg A, Brown RL. A study of the failure of concrete under combined compressive stress. Urbana: University of Illinois Bulletin; 1928.
- Richart FE, Brandtzaeg A, Brown RL. The failure of plain and spirally reinforced concrete in compression. Urbana: University of Illinois Engineering Experiment Station Bulletin no. 190; 1929.
- Mander JB, Priestley MJN, Park R. Observed stress–strain behavior of confined concrete. *J Struct Eng*. 1988;114(8):1827–49.
- Mander JB, Priestley MJN, Park R. Theoretical stress–strain model for confined concrete. *J Struct Eng*. 1988;108(12):2703–22.
- Saatcioglu M, Razvi SR. Circular high-strength concrete columns under concentric compression. *ACI Struct J*. 1999;96(5):1438–47.
- Assa B, Nishiyama M, Watanabe F. New approach for modeling confinement concrete I: circular columns. *J Struct Eng*. 2001;127(7):743–50.
- Montgomery DL. Behavior of spirally reinforced high strength concrete columns under axial loading. Doctoral and master thesis. National Library of Canada. 1996.
- Baduge SK, Mendis P, Ngo T, Portella J, Nguyen K. Understanding failure and stress–strain behavior of high strength concrete (> 100 MPa) confined by lateral reinforcement. *Constr Build Mater*. 2018;189(20):62–77.
- Cusson D, Paultre P. Stress–strain model for confined high-strength concrete. *J Struct Eng*. 1995;121(3):468–77.
- Razvi SR, Saatcioglu M. Tests of high-strength concrete columns under concentric loading. Report no. OCCEERC 96-03, Ottawa Caeleton Earthquake Engineering Research Centre, Ottawa, ON, Canada, 1996.
- Yang X, Zohrevamnd P, Mirmiran A. Behavior of ultra-high-performance concrete confined by steel. *J Mater Civ Eng*. 2016;28(10):04016113.
- Chen MY, Zheng WZ, Hou XM. Experimental study on mechanical behavior of RPC circular columns confined by high strength stirrups under axial compression. *Funct Mater*. 2017;24(1):82–90.
- Ministry of Housing and Urban-rural Development of the People’s Republic of China, GB/T 50010-2010: Code for design of concrete structures. China Ministry of construction. Beijing: China Architecture and Building Press. 2010.
- China Standardization Administration, GB/T 31387-2015: Reactive Powder Concrete. China Standardization Administration, Beijing: China Standard Press, 2015.
- China Standardization Administration, GB/T 228.1-2012: Metallic materials-tensile testing—part 1: methods of test at room temperature. China Standardization Administration, Beijing: China Standard Press. 2012.
- Ministry of Housing and Urban-rural Development of the People’s Republic of China, GB/T 50512-2012: Standard for test

- method of concrete structures. China Ministry of construction. Beijing: China Architecture and Building Press. 2012.
24. Guo ZH, Zhang XQ, Zhang DC, Wang RQ. Experimental investigation of the complete stress–strain curve of concrete. *J Build Struct*. 1982;01:1–12.
  25. Sharma UK, Bhargava P, Kaushik SK. Behavior of confined high strength concrete columns under axial compression. *J Adv Concr Technol*. 2005;3(2):267–81.
  26. Foster SJ, Attard MM. Experimental tests on eccentrically loaded high strength concrete columns. *ACI Struct J*. 1997;94(3):295–302.
  27. Légeron F, Paultre P. Uniaxial confinement model for normal- and high strength concrete columns. *J Struct Eng*. 2003;129(2):241–52.
  28. Wang N, Shi QX, Zheng W, Zheng GD, Wang HL. A uniaxial compressive model for concrete confined with stirrups. *J Build Mater*. 2019;22(6):933–40.
  29. Wei Y, Wu YF. Compression behavior of concrete columns confined by high strength steel wire. *Constr Build Mater*. 2014;54:443–53.
  30. Sheikh SA, Uzumeri SM. Strength and ductility of tied concrete columns. *J Struct Eng*. 1980;106(5):1079–102.
  31. Yang K, Shi QX, Jiang WS. Calculation of high-strength lateral ties stress of high-strength confined concrete. In: *The 10th national academic conference on basic theory and engineering application of concrete structures*, Dalian. 2009. p. 421–6.
  32. Saatcioglu M, Razvi SR. Strength and ductility of confined concrete. *J Struct Eng*. 1992;118(6):1590–607.
  33. Guralnick SA, Gunawan L. Design of concrete members subjected to triaxial compression. *Pract Period Struct Des Constr*. 2009;14(1):43–9.
  34. Foster SJ, Attard MM. Strength and ductility of fiber-reinforced high-strength concrete columns. *J Struct Eng*. 2001;127(1):28–34.
  35. Zaina M, Foster SJ. Testing of concentric and eccentrically loaded fiber-reinforced HSC columns. Sydney: School of Civil and Environmental Engineering, University of New South Wales; 2005.
  36. Shin HO, Min KH, Mitchell D. Confinement of ultra-high performance fiber reinforced concrete columns. *Compos Struct*. 2017;176:124–42.
  37. Hong KN, Han SH, Yi ST. High-strength concrete columns confined by low-volumetric-ratio lateral ties. *Eng Struct*. 2006;28(9):1346–53.
  38. Hong KN, Akiyama M, Yi SY, Suzuki M. Stress–strain behavior of high-strength concrete columns confined by low-volumetric ratio rectangular ties. *Mag Concr Res*. 2006;58(2):101–15.
  39. Cusson D, Paultre P. High-strength concrete columns confined by rectangular ties. *J Struct Eng*. 1998;120(3):783–804.
  40. Chung HS, Yang KH, Lee YH, Eun HC. Stress–strain curve of laterally confined concrete. *Eng Struct*. 2002;24(9):1153–63.
  41. Li YZ, Cao SY, Liang H, Ni XY, Jing DH. Axial compressive behavior of concrete columns with grade 600 MPa reinforcing bars. *Eng Struct*. 2018;172(1):497–507.
  42. Antonius A, Imran I, Setiyawan P. On the confined high-strength concrete and need of future research. *Proceed Eng*. 2017;2017(171):121–30.
  43. Saatcioglu M, Razvi SR. High-strength concrete columns with square sections under concentric compression. *J Struct Eng*. 1998;124(12):1438–47.

**Publisher's Note** Springer Nature remains neutral with regard to jurisdictional claims in published maps and institutional affiliations.